# PLOS ONE

# A convenient approach to synthesize substituted 5-Arylidene-3-*m*-tolyl thiazolidine-2, 4-diones by using morpholine as a catalyst and its theoretical study

**Khorshada Jahan*⊕, Kaif Rashid Khan⊕, Kawsari Akhter*, Umme Kulsum Rowzatur Romman, Ershad Halim**

Department of Chemistry, University of Dhaka, Dhaka, Bangladesh

⊕ These authors contributed equally to this work.
* khorshada26@gmail.com (KJ); kawsariakhter@yahoo.com (KA)
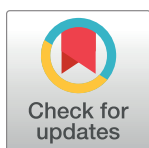
## Abstract

Thiazolidinediones are very important and used as a drug for the treatment of type 2 diabetes. Here, we report a convenient approach to synthesis 3-m-tolyl-5-arylidene-2,4-thiazolidinediones (TZDs) derivatives **7a-e** in two steps with moderate to good yield using morpholine as a catalyst. All the structures were confirmed by their spectral IR, $^1$H NMR and $^{13}$C NMR data. The anti-diabatic activity of all synthesized molecules is evaluated by docking with peroxisome proliferator-activated receptor-γ (PPARγ). Preliminary flexible docking studies reveals that our compounds **7a**, **7d** and **7e** showed better binding affinity with the protein and could be a potential candidate for the treatment of type 2 diabetes in near future.

## Introduction

Heterocyclic compounds play an important role in medicinal chemistry. Specifically, nitrogen-containing heterocycles with a sulfur atom such as, thiazolidine-2,4-dione (TZDs, **Fig 1**). TZDs represent an important class of compounds showed a wide spectrum of biological and pharmacological activities [1,2]. In the past decades, TZDs have been the subject of extensive research because of their involvement in the regulation of different physiological processes which has been confirmed by numerous reviews [3,4]. A variety of compounds having TZDs core (**Fig 1**) were used for the treatment of type II diabetes and related diseases [5]. Thiazolidinediones showed antidiabetic activity by binding with gamma form of the peroxisome proliferator-activated receptor-γ (PPARγ). This stimulates peripheral adiposities to increase their uptake of free fatty acids, which leads to reduction in the fat stored in muscles, liver and visceral fat deposits. The TZDs also leads to an increase in the secretion of adiponectin and a decrease in the production of inflammatory mediators such as tumor necrosis factor-alpha (TNF-α), plasminogen activator inhibitor-1(PAI-1) and interleukin-6 (IL-6). This feature lead TZDs act as an aldose reductase inhibitor and tumor inhibitor [6,7]. Moreover, chemical modification on this heterocycle led to a class of compounds that possess several biological activities including, anti-inflammatory effects [8], antibacterial [9–12], antitubercular [13], and antifungal activity [9]. TZDs
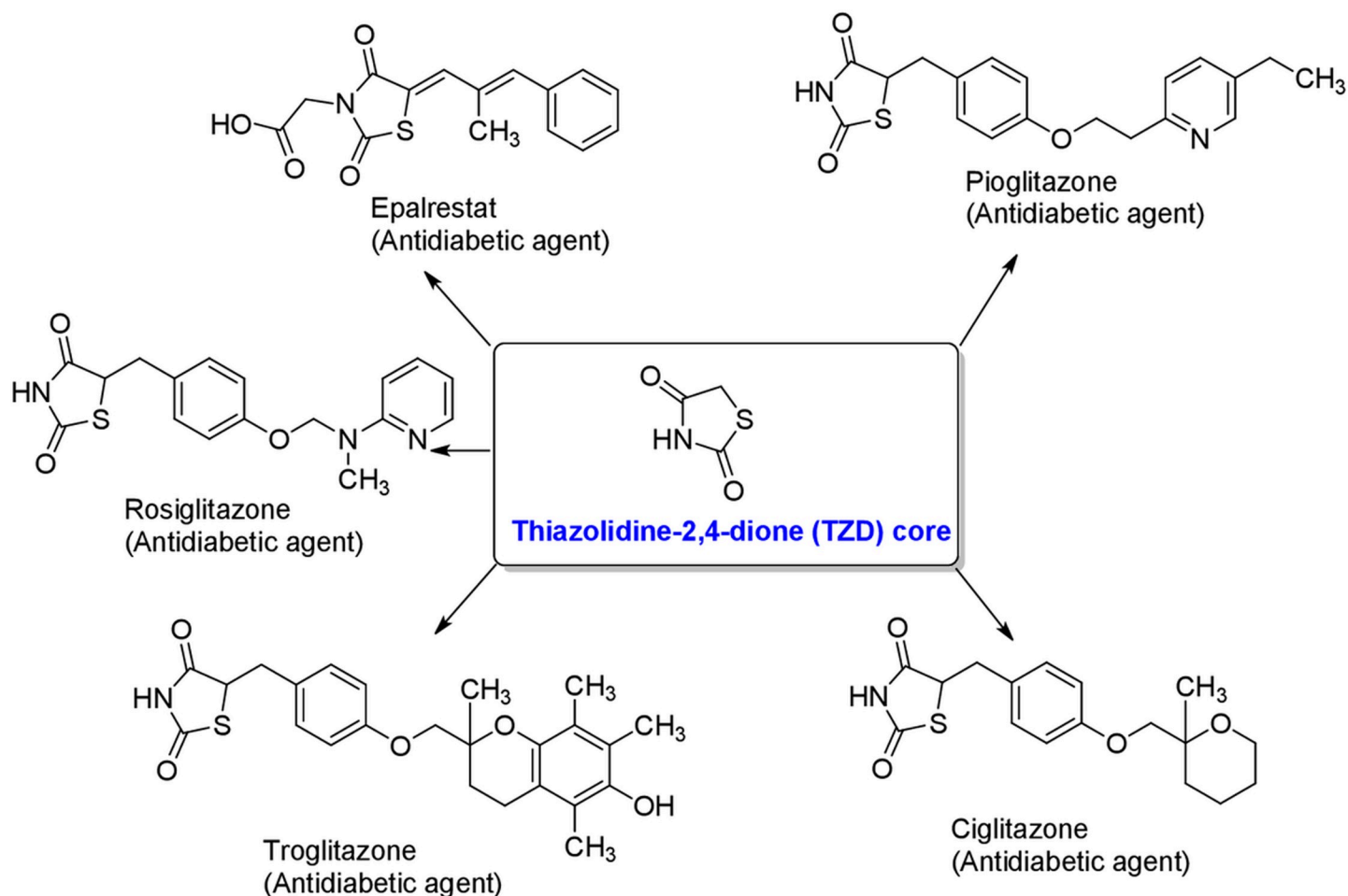
**Fig 1. Thiazolidine-2,4-dione (TZD) and its derivatives.**

target vascular cells and monocytes/macrophages to inhibit the production of pro-inflammatory cytokines [14–17] as well as the development of oxidative stress [18] and cell adhesion molecules. They are also key intermediates for the synthesis of anti-HIV and anti-ischemic agents [19–21]. Therefore, simple structure and valuable pharmacological activity of these molecules gained special attention from synthetic chemists and pharmacologists [20].

Several methods have been reported up to date for the synthesis of thiazolidine-2,4-dione and its derivatives with an extensive range of catalysts including Alum [22], glycine, sodium carbonate, piperidinium acetate [23], piperidine [24], amines salts [25], baker's yeast [26], ionic liquids [27–31] and nanoparticle-supported copper (II) catalysts [32]. However, several of these existing methods suffer from one or more drawbacks, such as low yields, long reaction times, environmentally unfavorable solvents, and a requirement for excess catalyst. Hence, a facile efficient process is still desirable. As a continuation our research goal to develop a convenient method to synthesize valuable synthon [33–36] from easily available starting materials, we developed a two-step method to synthesize thiazolidine-2,4-dione derivatives by using morpholine as a catalyst. We have performed Density functional theory (DFT) calculations in all our synthesized molecules to find out most active compound. To the best of our knowledge, the use of morpholine as a catalyst for the synthesis of 3-*m*-tolyl-5-arylidenthiazolidine-2,4-diones as well as DFT calculations has not been previously reported.

## Experimental

### Chemistry

**General.** All products were characterized by IR, UV, $^1$H-NMR and $^{13}$C-NMR. Thin layer chromatography (TLC) was carried out on plates coated with silica gel (Merck, Silica Gel G) and spots were detected with iodine vapour. The UV spectra was recorded using SHIMADZU UV-160A spectrophotometer using chloroform as solvent. Infra-Red spectra was recorded using SHIMADZU IR-470A spectrophotometer by direct transmittance using KBr pellets. Multinuclear NMR ($^1$H, $^{13}$C, DEPT-135) spectra were recorded on a BRUKER 400 MHz NMR spectrophotometer. Chemical shifts are reported in parts per million (ppm). Tetramethyl silane (TMS) served as an internal standard in $^1$H and $^{13}$C NMR (δ 0.00 ppm). All the chemicals used for the synthesis of target compounds have been purchased from Sigma Aldrich and were used as received. Scanned Spectra for all compounds are shown in **S1–S29 Figs.**

**General procedure for the synthesis of 3-(*m*-tolyl)thiazolidine-2,4-dione (4).** A solution of *m*-tolylthiourea, (**1**, 5.0g, 30.0 mmol), 2-chloroacetic acid, (**2**, 2.8 g, 30.0 mmol) and 20mL hydrochloric acid **3** (30%, (v/v)) were stirred for half an hour and then refluxed for overnight at 120˚C in a 250mL round-bottomed flask. After completion of the reaction, as monitored by TLC (2:1, Pet ether: Ethyl acetate), the reaction mixture was gradually cooled to room temperature. Then it was neutralized with dilute sodium hydroxide (0.1 M). Immediately a solid mass was formed which was filtered under reduce pressure, washed with cold water (50mL) and recrystallized from absolute alcohol to give a pure product **4** as a white crystal (2.49g, 40% yield).

**General procedure for the synthesis of 5-arylidene-3-(*m*-tolyl)-thiazolidine-2,4-diones (7a-e).** For each experiment, 20mmol of compound **4** and 20 mmol of substituted benzaldehydes **5a-e** was dissolved in absolute alcohol (10 mL) and refluxed with the Dean-Stark attachment for 2 hours by using morpholine **6** (10 mol%) as a catalyst. After completion of the reaction, as judged by TLC, the reaction was quenched with crushed ice. The crude product was filtered under reduced pressure, washed with cold water and purified by recrystallization using absolute alcohol. The yield of the products **7a-e** ranged from 55–90%.

**Spectral data.** *3-(m-tolyl) thiazolidine-2, 4- dione, Compound (4)*. Yield: 40%; R$_f$: 0.81; white crystal; UV (λ$_{max}$ nm): 274.50; IR (KBr) (ν$_{max}$ cm$^{-1}$): 1760, 1688 (C = O, TZD ring), 1521, 1198 (-CH$_2$ stretch), 761; $^1$H NMR (CDCl$_3$, 400MHz, δ ppm): 7.43–7.32 (m, 3H), 7.13 (d, *J* = 7.6 Hz, 1H), 4.17 (d, *J* = 1.6 Hz, 2H), 2.203, (s, 3H); $^{13}$C NMR (CDCl$_3$, 100MHz, δ ppm): 170.56, 170.43, 136.00, 131.97, 131.36, 130.09, 128.28, 127.25, 33.99, 17.52.

*5-(2-Methoxybenzylidene)-3-m-tolyl thiazolidine-2, 4- dione (7a)*. Yield: 84% (morpholine 11%); R$_f$: 0.34; yellow crystals; UV (λ$_{max}$ nm): 358.50; IR (KBr) (ν$_{max}$ cm$^{-1}$): 1742, 1690 (C = O, TZD ring); $^1$H NMR (CDCl$_3$, 400 MHz, δ ppm): 8.37 (s, 1H), 7.54–6.99 (m, 7H), 3.94 (s, 3H), 2.24 (s, 3H); $^{13}$C NMR (CDCl$_3$, 100 MHz, δ ppm): 167.43, 165.61, 158.56, 136.26, 132.39, 132.13, 131.29, 130.47, 130.33, 129.94, 129.53, 128.43, 127.14, 121.31, 120.94, 111.23, 55.54, 17.65.

*5-(2-Chlorobenzylidene)-3-m-tolyl thiazolidine-2, 4- dione (7b)*. Yield: 88%; R$_f$: 0.50; green crystals; UV (λ$_{max}$ nm): 358.50; IR (KBr) (ν$_{max}$ cm$^{-1}$): 1734, 1675 (C = O, TZD ring); $^1$H NMR (CDCl$_3$, 400 MHz, δ ppm): 8.35 (s, 1H), 7.65–7.21 (m, 7H), 2.26 (s, 3H); $^{13}$C NMR (CDCl$_3$, 100 MHz, δ ppm): 166.59, 164.92, 136.20, 136.06, 131.85, 131.80, 131.47, 131.37, 130.69, 130.54, 130.11, 128.35, 127.34, 127.22, 124.42, 17.66.

*5-(2-Nitrobenzylidene)-3-m-tolyl thiazolidine-2, 4- dione (7c)*. Yield: 67%; R$_f$: 0.22; light brown crystals; UV (λ$_{max}$ nm): 332.00 and 243.50; IR (KBr) (ν$_{max}$ cm$^{-1}$): 1690, 1607 (C = O TZD ring), 1352(-NO$_2$); $^1$H NMR (CDCl$_3$, 400 MHz, δ ppm): 7.99 (s, 1H), 7.50–7.20 (m, 7H), 2.45 (s, 3H); $^{13}$C NMR (CDCl$_3$, 100 MHz, δ ppm): 166.97, 165.63, 141.47, 136.23, 134.60, 132.03, 131.33, 130.53, 130.39, 130.06, 130.01, 127.19, 120.07, 17.64.

*5-(3-Hydroxybenzylidene)-3-m-tolyl thiazolidine-2, 4- dione, Compound (7d)*. Yield: 54%; $R_f$: 0.45; dark-brown powder; UV ($\lambda_{max}$ nm): 328.00;; $^1$H NMR (CDCl$_3$, 400 MHz, δ ppm): 7.96 (s, 1H), 7.53 (s, 4H), 7.51–7.35 (m, 3H), 7.22–7.19 (d, $J$ = 7.6 Hz, 1H), 2.24 (s, 3H); $^{13}$C NMR (CDCl$_3$, 100 MHz, δ ppm): 166.36, 165.32, 136.83, 136.18, 132.95, 131.87, 131.73, 131.39, 130.13, 129.64, 128.36, 127.25, 121.97, 17.63.

*5-(4-Chlorobenzylidene)-3-m-tolyl thiazolidine-2, 4- dione, Compound (7e)*. Yield: 74%; $R_f$: 0.12; off-white crystals; UV ($\lambda_{max}$ nm): 334.50; IR (KBr) ($\nu_{max}$ cm$^{-1}$): 1857 and 1783 (C = O TZD ring); $^1$H NMR (CDCl$_3$, 400 MHz, δ ppm): 7.96 (s, 1H), 7.52 (s, 4H), 7.43–7.37 (m, 3H), 7.21–7.19 (d, $J$ = 7.6 Hz, 1H), 2.24 (s, 3H); $^{13}$C NMR (CDCl$_3$, 100 MHz, δ ppm): 166.37, 165.32, 136.85, 136.17, 132.96, 131.84, 131.72, 131.38,131.36, 130.12, 129.64, 128.34, 127.24, 121.96, 17.61.

## Computational methods

**DFT studies.**   All theoretical calculations were performed by using density functional theory (DFT), B3LYP (6-31G, d) basis set in Gaussian 09 Program suite. A full geometry optimization was performed for all structures, using this function and all geometries were visualized using Avogadro 1.2 software package.

**Preparation of the protein.**   Crystal structure of human peroxisome proliferator-activated receptor gamma (PPARγ) [37] (PDB ID: 3GBK) was downloaded from RCSBPDB webpage (www.rcsb.org) and opened on PyMol (version 1.3) and waters and the agonist were removed from the crystal structure. The protein structure was then subjected to geometry and energy minimization in Swiss-PDBViewer (version 4.1.0) using GROMOS96 force field. The crystal structure of the protein after energy minimization was shown in Fig 2. The crystal structure was then saved as a.pdb file and used for molecular docking against the optimized structures of **4** and **7a-e**.

**Molecular docking.**   Docking of the optimized structures were performed against 3GBK using AutoDock Vina. As a control, the commercially available type 2 anti-diabatic drug, Epalrestat was used. Only flexible docking was performed where the ligands were flexible, but the protein was held rigid. The dimension of the grid-box for the protein was set to 73.5450, 60.6299, 79.5208 Å as the X-, Y- and Z-coordinates respectively. After docking, all generated files were collected and their non-covalent interactions with the energy minimized protein was evaluated in Accelerys Discovery Studio 4.

## Results and discussion

### Chemistry

The synthesis of the new TZD derivatives had two steps. At first phenyl thiourea **1** reacts with chloroacetic acid **2** in the presence of hydrochloric acid **3** (30 mol%, (v/v)) as a catalyst to produce the desired 3-(*m*-tolyl) thiazolidine-2,4-dione **4**. Then the active methylene in position 5 of compound **4** undergo Knoevenagel condensations with various aromatic aldehydes **5a-e** in the presence of morpholine **6** to form compounds **7a–e** (S33 Fig). The yield in the first step is low because of the presence of unreacted starting material and formation of potential by product 3-toluidine (mechanism presented in **S30 Fig**). In second step, it should be noted that both electron-withdrawing and electron-donating groups in aromatic aldehydes are quite suitable and give the desired product good to moderate yield, except compound **7d**, where the presence of hydroxy group, the reaction become sluggish and it is difficult to separate the product.

After completing the reaction, all the products are recrystallized by using suitable solvent and checked by TLC. All the structures were confirmed by their spectral data (IR, UV, $^1$H NMR, and $^{13}$C NMR). In compound **4**, the IR spectra exhibited characteristic absorption
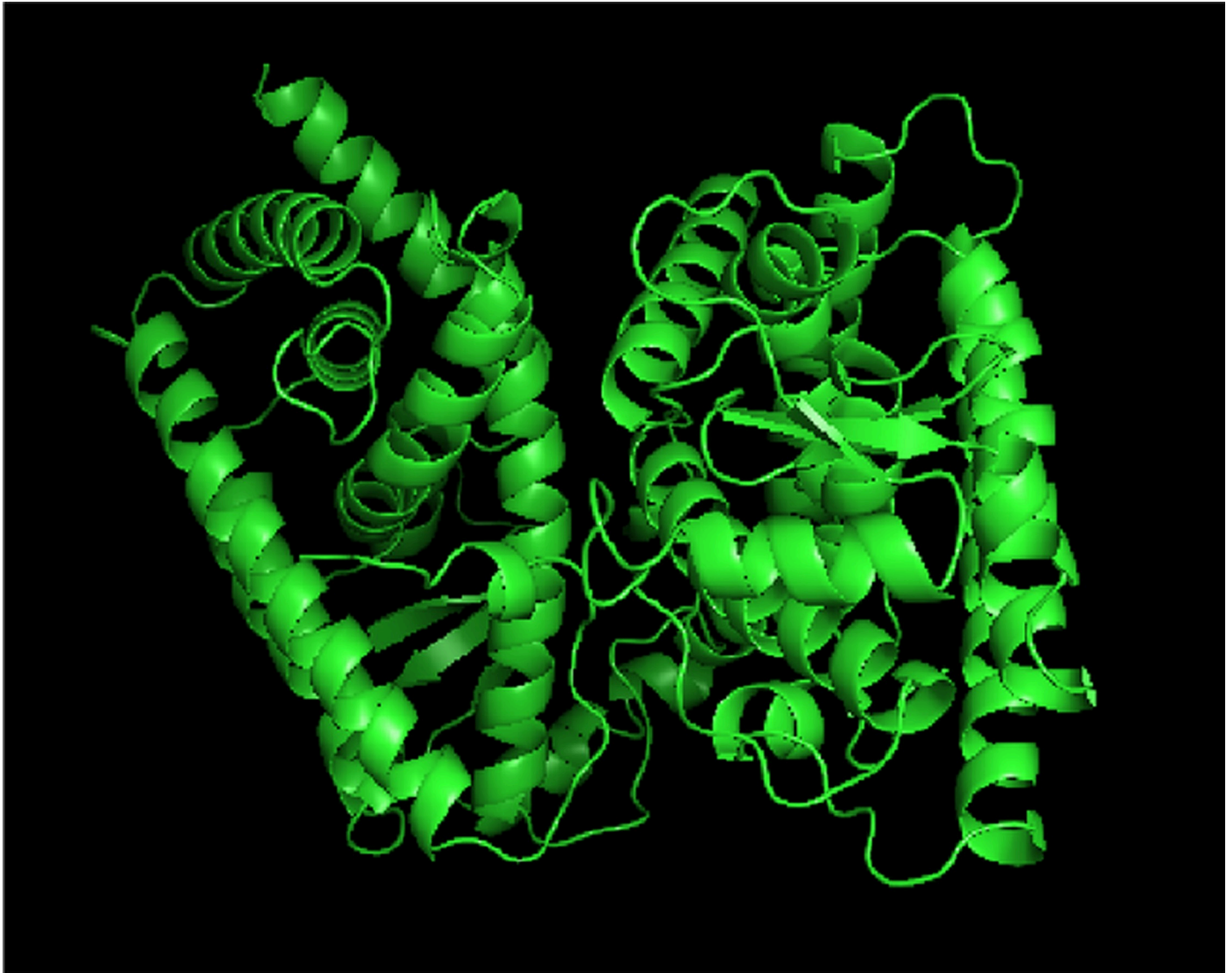
**Fig 2. The X-ray crystal structure of PPARγ (PDB ID: 3GBK).**

bands at 1680–1690 cm$^{-1}$ and 1755–1765 cm$^{-1}$ due to the two C = O from the TZD heterocycle. The $^1$H NMR spectra showed characteristic doublets due to presence of C (5)-H in compound **4** at 4.169 and 4.173 ppm respectively which is further confirmed by DEPT spectra shown is **S5 Fig**. The condensation reaction between **4** and **5** formed compound **7**, where The C (5)–H in thiazole disappeared and a characteristic peak appeared around 8.0 ppm indicate the conversion of the methylene group to C = C double bond. Both $^{13}$C NMR and DEPT-135 data supported the conversion of the methylene group to C = C double bond.

## DFT studies: Thermodynamic results

Compounds **4** and **7a-e** were optimized to obtain their most thermodynamically favorable configuration where Epalrestat was used as a control compound. The thermodynamic data of all synthesized compounds have negative electronic energy, enthalpy and Gibbs-free energy

**Table 1. Theoretical thermodynamic results of Epalrestat, compound 4 and 7a-e.**

| Compound | Internal Energy, E | Enthalpy, ΔH | Free energy, ΔG | Dipole Moment, μ (D) |
|---|---|---|---|---|
| Epalrestat | -1333.010 | -1333.009 | -1333.080 | 5.5006 |
| 4 | -989.721 | -989.720 | -989.774 | 1.0328 |
| 7a | -1373.259 | -1373.258 | -1373.332 | 4.1495 |
| 7b | -1718.372 | -1718.371 | -1718.443 | 3.0389 |
| 7c | -1463.259 | -1463.258 | -1463.333 | 5.1613 |
| 7d | -1333.984 | -1333.983 | -1334.053 | 1.3643 |
| 7e | -1718.376 | -1718.375 | -1718.446 | 0.4355 |

suggesting that all the synthesized molecules are thermodynamically stable (Table 1). Compound 4 is thermodynamically less stable than compared to the other compounds 7a-e including Epalrestat. In compounds 7a-e, all compounds have similar energy except 7b and 7e which have lower energy because of the presence of Cl atom, hence, more stable. It should be noted that compounds 7a-e after Knoevenagel condensation develop an alkene bond which stabilized the molecule by delocalized pi-orbitals hence favor lower energy. In order to find out the binding energy and hydrogen bonding capability, the dipole moment of all synthesized compounds was determined (S31 Fig and Table 1). The range of dipole moment for the synthesized molecules is in between 0.5–5.5 Debye, where 7e has the lowest dipole moment because of the presence chlorine atom at *para*-position and most for Epalrestat because it contains polar groups such as a carboxyl.

**Electrostatic results.** To find out the reactivity of the molecule towards its receptor, HOMO-LUMO and hardness and softness of all synthesized molecules were calculated (S32 Fig and Table 2). In the Frontier molecular orbital, large energy gap between HOMO-LUMO indicates that the molecule is more stable and less reactive, where low energy gap suggests easier electronic transition and favor quicker reaction. All the synthesized compounds 7a-e except compound 4 have similar orbital energy gap suggesting similar reactivity towards its receptor.

## Docking studies

Binding affinity is a measure of how strongly a molecule can fit into a receptor and interact with it through non-covalent bonding. To find out the binding affinity as well as protein interaction, we performed docking of all our synthesized compounds 4 and 7a-e with Peroxisome proliferator-activated receptor gamma (PPAR-γ or PPARG) by considering Epalrestat as a reference (Figs 3–9 and Table 3). In result, three compounds 7a, 7d and 7e showed better binding affinity with the protein having energy -8.2, -8.5 and -8.9 kcal/mol respectively than compared to Epalrestat which has a binding affinity of -7.9 kcal/mol and hence showed better non-covalent interactions. Compound 4 has -6.9 kcal/mol of energy when bound to the

**Table 2. Theoretical electrostatic results of Epalrestat, compound 4 and 7a-e.**

| Compounds | HOMO (a.u) | LUMO (a.u) | Orbital energy gap (a.u) | Softness | Hardness |
|---|---|---|---|---|---|
| Epalrestat | -0.21876 | -0.08698 | 0.13178 | 15.177 | 0.06589 |
| 4 | -0.24558 | -0.03353 | 0.21205 | 9.4312 | 0.10603 |
| 7a | -0.21447 | -0.07913 | 0.13534 | 14.778 | 0.06767 |
| 7b | -0.23280 | -0.08768 | 0.14512 | 13.782 | 0.07256 |
| 7c | -0.24179 | -0.10205 | 0.13929 | 14.358 | 0.06965 |
| 7d | -0.22289 | -0.08649 | 0.13640 | 14.663 | 0.06820 |
| 7e | -0.22956 | -0.09098 | 0.13858 | 14.432 | 0.06929 |

**Fig 3. 2D-representation of the non-covalent interactions of Epalrestat with receptor (3gbk) after flexible docking.**

https://doi.org/10.1371/journal.pone.0247619.g003



**Fig 4. 2D-representation of the non-covalent interactions of 4 and receptor (3gbk) after flexible docking.**

https://doi.org/10.1371/journal.pone.0247619.g004



**Fig 5. 2D-representation of the non-covalent interactions of 7a with receptor (3gbk) after flexible docking.**

https://doi.org/10.1371/journal.pone.0247619.g005
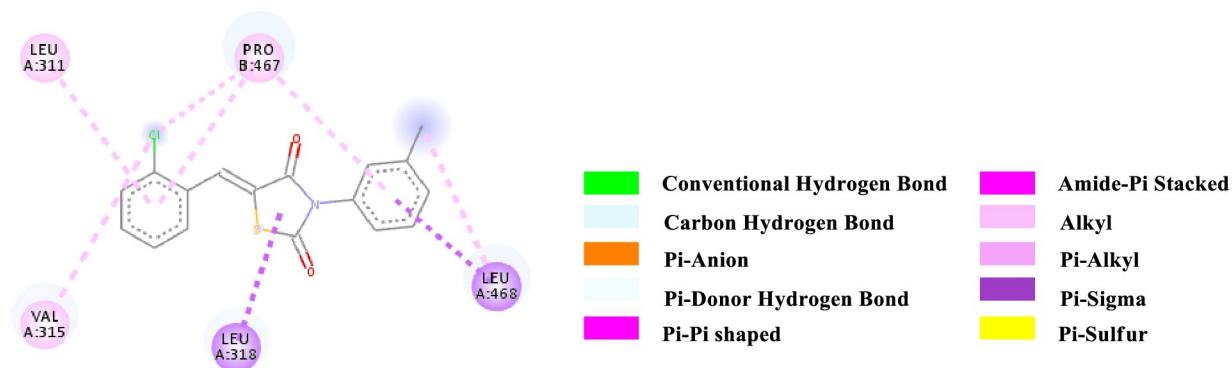
**Fig 6. 2D-representation of the non-covalent interactions of 7b with receptor (3gbk) after flexible docking.**

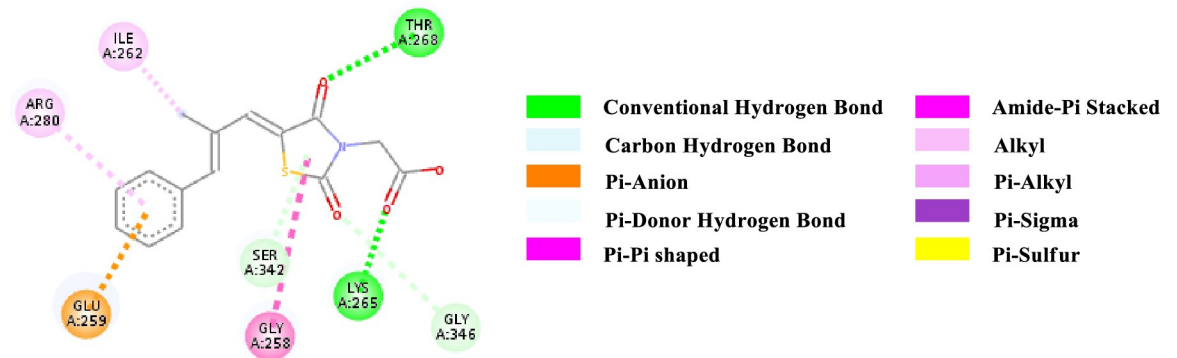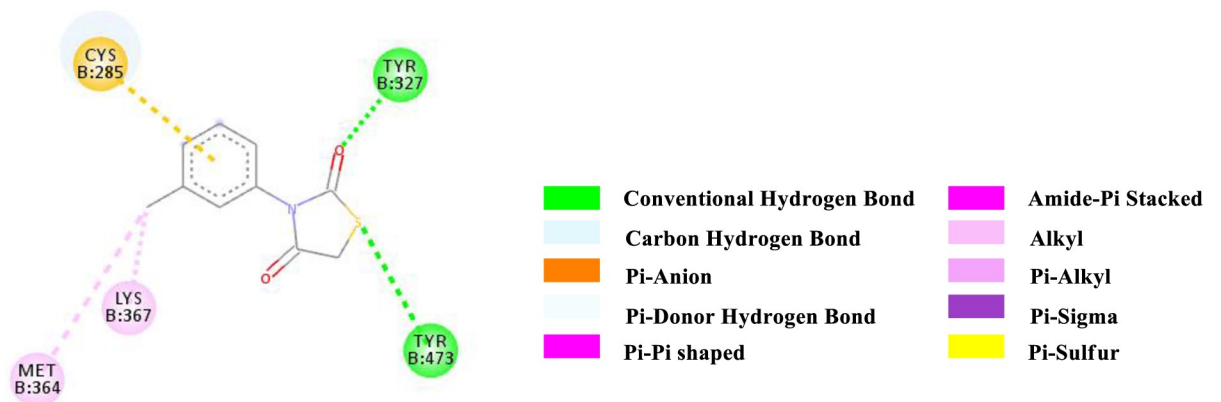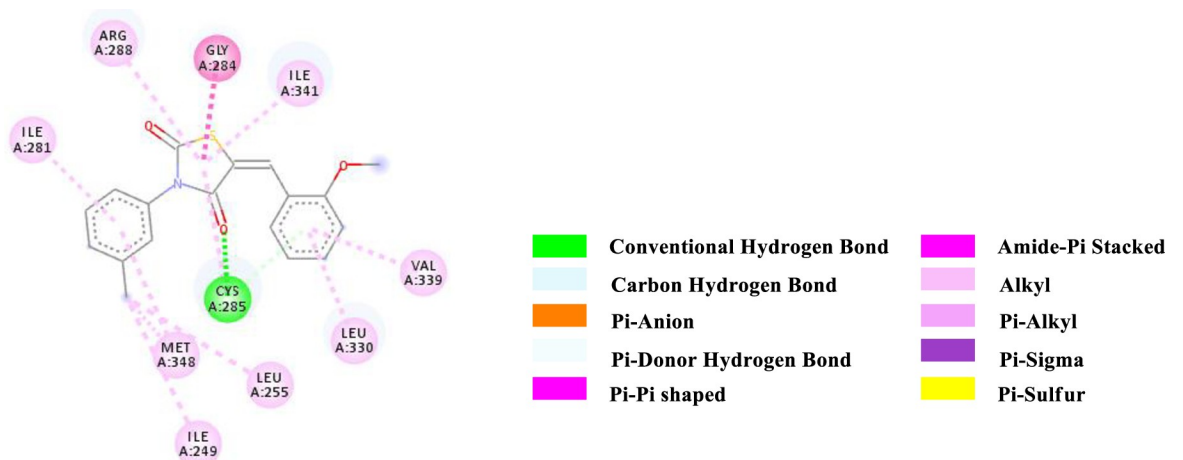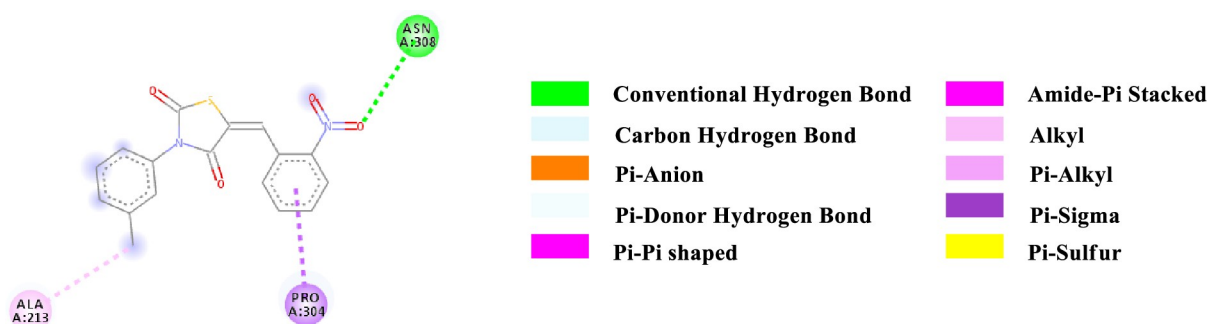**Fig 7. 2D-representation of the non-covalent interactions of 7c with receptor (3gbk) after flexible docking.**
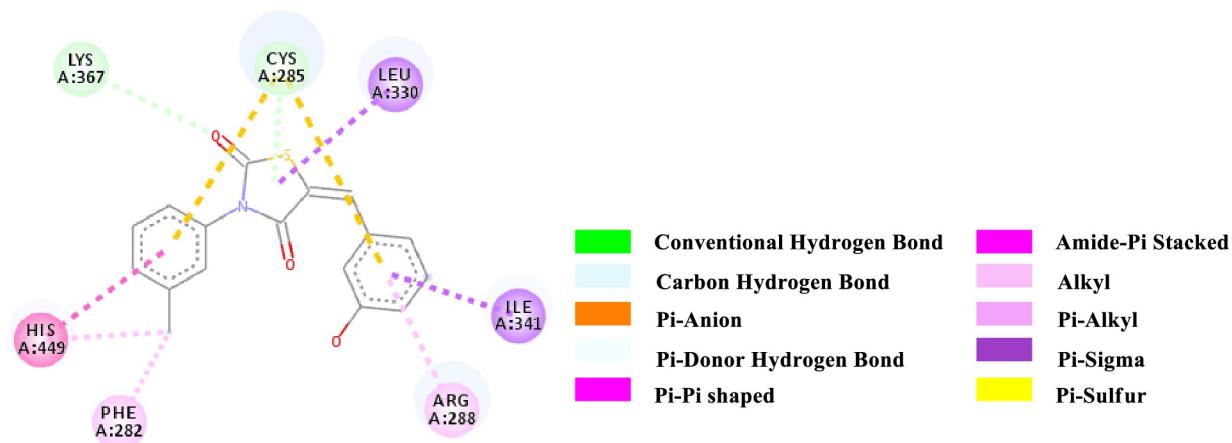
**Fig 8. 2D-representation of the non-covalent interactions of 7d with receptor (3gbk) after flexible docking.**

receptor. This result indicates that the binding pocket of the protein is quite large so the structure bigger than **4** would have more interactions when bound to the protein. This was true for all our compounds **7a-e** which had higher binding affinity than **4**. However, Compound **7b** and **7c** have lower binding affinity than Epalrestat which indicate that the ortho position may

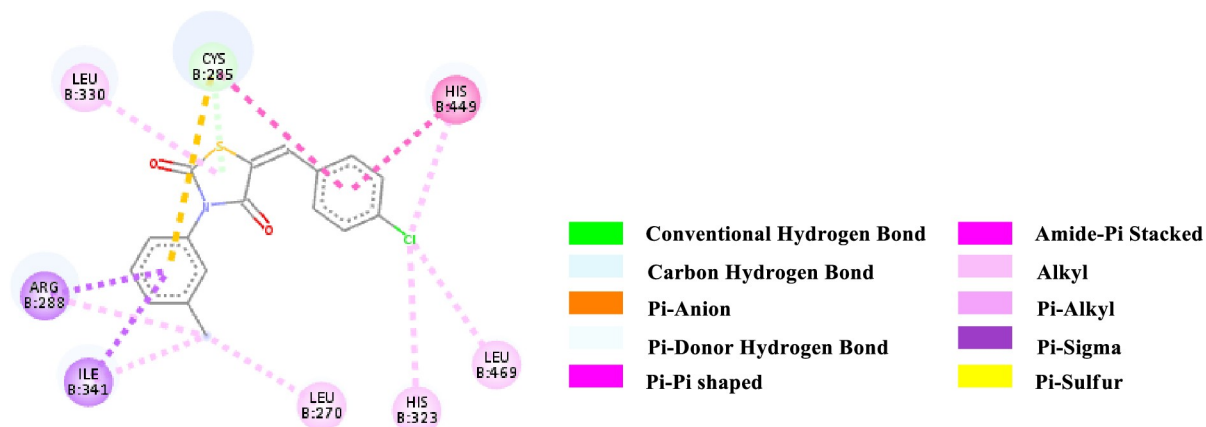**Fig 9. 2D-representation of the non-covalent interactions of 7e with receptor (3gbk) after flexible docking.**

https://doi.org/10.1371/journal.pone.0247619.g009

not be a good site for better binding affinity. Only exception was observed with **7a,** where the methoxy group at ortho-position had no interaction with the protein. This result suggests that a good choice in a substituent may induce better binding. Compound **7e** has better binding

**Table 3. Binding affinities and types of non-bonding interactions of the optimized ligands Epalrestat, compound 4 and 7a-e with the protein.**

| Compounds | Binding Affinity, kcal/mol | Type of Non-bonding Interaction | From | To | Bond Distance, Å |
|---|---|---|---|---|---|
| Epatrestat | -7.9 | HB | Lys 265 (NH) | C = O (ligand) | 3.06067 |
| | | HB | Thr 268 (OH) | C = O (4th position of TZD) | 3.21220 |
| | | CHB | Gly 346 (αCH) | C = O (2nd position of TZD) | 3.64643 |
| | | PA | Glu 259 (COO-) | Benzene (ligand) | 3.64293 |
| | | PDHB | Ser 342 (OH) | TZD core | 3.72507 |
| | | APS | Gly 258—Glu 259 (CONH) | TZD core | 4.20658 |
| | | Alkyl | Methyl (ligand) | Ile 262 (side chain) | 5.38888 |
| | | Pi-Alkyl | Benzene (ligand) | Arg 280 (side chain) | 4.88631 |
| 4 | -6.1 | HB | Tyr 327 (OH) | C = O (2nd position of TZD) | 3.12856 |
| | | HB | Tyr 473 (OH) | TZD (Sulfur) | 3.31594 |
| | | PS | Cys 285 (SH) | N-Aryl (ligand) | 4.25927 |
| | | Alkyl | Methyl (N-Aryl, ligand) | Met 364 (side chain) | 5.29768 |
| | | Alkyl | Methyl (N-Aryl, ligand) | Lys 367 (side chain) | 4.27732 |
| 7a | -8.2 | HB | Cys 285 (SH) | C = O (4th position of TZD) | 3.71078 |
| | | PDHB; PS | Cys 285 (SH) | 2-OMe (Aryl); TZD core (ligand) | 4.11671 |
| | | APS | Gly 284; Cys 285 (CONH) | TZD core (ligand) | 3.90759 |
| | | Alkyl | Methyl (Aryl; ligand) | Ile 249 (side chain) | 4.68460 |
| | | Alkyl | Methyl (Aryl; ligand) | Leu 255 (side chain) | 5.06828 |
| | | Alkyl | Methyl (Aryl; ligand) | Met 348 (side chain) | 5.05667 |
| | | Pi-Alkyl | 2-OMe (Aryl; ligand) | Cys 285 (side chain) | 5.40245 |
| | | Pi-Alkyl | TZD core (ligand) | Arg 288 (side chain) | 4.94846 |
| | | Pi-Alkyl | TZD core (ligand) | Ile 341 (side chain) | 4.27639 |
| | | Pi-Alkyl | 2-OMe (Aryl; ligand) | Leu 330 (side chain) | 4.87080 |
| | | Pi-Alkyl | 2-OMe (Aryl; ligand) | Val 339 (side chain) | 5.01580 |
| | | Pi-Alkyl | N-Aryl (ligand) | Ile 281 (side chain) | 4.99136 |
| | | Pi-Alkyl | N-Aryl (ligand) | Met 348 (side chain) | 5.24193 |

(*Continued*)

**Table 3.** (Continued)

| Compounds | Binding Affinity, kcal/mol | Type of Non-bonding Interaction | From | To | Bond Distance, Å |
|---|---|---|---|---|---|
| **7b** | -7.3 | PS | Leu 318 (Methyl, side chain) | TZD core (ligand) | 3.63093 |
| | | PS | Leu 468 (Methyl, side chain) | N-Aryl (ligand) | 3.63461 |
| | | PS | Leu 468 (Methyl, side chain) | N-Aryl (ligand) | 3.96613 |
| | | Alkyl | 2-Cl-Aryl (ligand) | Val 315 (side chain) | 5.14187 |
| | | Alkyl | 2-Cl-Aryl (ligand) | Pro 467 (side chain) | 4.68961 |
| | | Alkyl | Methyl (N-Aryl, ligand) | Leu 468 (side chain) | 4.69788 |
| | | Pi-Alkyl | 2-Cl-Aryl (ligand) | Leu 311 (side chain) | 5.49394 |
| | | Pi-Alkyl | 2-Cl-Aryl (ligand) | Pro 467 (side chain) | 5.44119 |
| | | Pi-Alkyl | N-Aryl (ligand) | Pro 467 (side chain) | 5.10571 |
| **7c** | -7.1 | HB | Asn 308 (NH$_2$) | 2-NO$_2$-Aryl (ligand) | 3.25728 |
| | | PS | Pro 304 ($\alpha$CH) | 2-NO$_2$-Aryl (ligand) | 3.77999 |
| | | Alkyl | Methyl (N-Aryl, ligand) | Ala 213 (side chain) | 4.46163 |
| **7d** | -8.5 | CHB | Lys 367 (side chain CH$_2$NH$_2$) | C = O (2nd position of TZD; ligand) | 3.70277 |
| | | PDHB; PS | Cys 285 (SH) | 3-OH-Aryl; TZD core (ligand) | 3.99461 |
| | | Pi-Sigma | Leu 330 (side chain) | TZD core (ligand) | 3.84019 |
| | | Pi-Sigma | Ile 341 (side chain) | 3-OH-Aryl (ligand) | 3.50391 |
| | | PS | Cys 285 (SH) | N-Aryl (ligand) | 5.46855 |
| | | PS | Cys 285 (SH) | 3-OH-Aryl (ligand) | 5.82541 |
| | | PPT | His 449 (Imidazole ring) | N-Aryl (ligand) | 4.96478 |
| | | APS | Cys 285; Gln 286 (CONH) | N-Aryl (ligand) | 5.20028 |
| | | Pi-Alkyl | 3-OH-Aryl (ligand) | Arg 288 (side chain) | 3.94502 |
| | | Pi-Alkyl | Phe 282 (Aryl) | Methyl (N-Aryl, ligand) | 4.90419 |
| | | Pi-Alkyl | His 449 (Imidazole ring) | Methyl (N-Aryl, ligand) | 4.80268 |
| **7e** | -8.9 | PDHB; PS | Cys 285 (SH) | N-Aryl; TZD core (ligand) | 3.68179 |
| | | Pi-Sigma | Arg 288 (side chain) | N-Aryl (ligand) | 3.55725 |
| | | Pi-Sigma | Ile 341 (side chain) | Methyl (N-Aryl, ligand) | 3.77542 |
| | | PS | Cys 285 (SH) | N-Aryl (ligand) | 5.46193 |
| | | PPT | His 449 (Imidazole ring) | 4-Cl-Aryl (ligand) | 4.67448 |
| | | APT | Cys 285; Gln 286 (CONH) | 4-Cl-Aryl (ligand) | 4.81318 |
| | | Alkyl | 4-Cl-Aryl (ligand) | Leu 469 (side chain) | 4.17882 |
| | | Alkyl | Methyl (N-Aryl, ligand) | Leu 270 (side chain) | 4.88063 |
| | | Alkyl | Methyl (N-Aryl, ligand) | Arg 288 (side chain) | 4.06932 |
| | | Alkyl | Methyl (N-Aryl, ligand) | Ile 341 (side chain) | 4.55730 |
| | | Pi-Alkyl | TZD core (ligand) | Leu 330 (side chain) | 4.65177 |
| | | Pi-Alkyl | 4-Cl-Aryl (ligand) | Cys 285 (side chain) | 5.15119 |
| | | Pi-Alkyl | His 323 (Imidazole ring) | 4-Cl-Aryl (ligand) | 4.39467 |
| | | Pi-Alkyl | His 449 (Imidazole ring) | 4-Cl-Aryl (ligand) | 5.03461 |

where *p*-Cl atom interacts with the protein. This finding suggests that adding larger groups in the *para* position may lead to higher binding affinity.

The various types of non-covalent interactions of each molecule with the receptor was shown in **Figs 3–9**. Most of the amino acids from the protein that have interacted with the synthesized compounds are either hydrophobic or basic. Hydrophobic interactions usually occurred from alkyl/pi-alkyl to amino acids such as Leu, His, Arg etc. There are a few polar interactions (hydrogen bond, carbon hydrogen bond and Pi-Donor hydrogen bond) as well as other interactions also occurred dependent on the electronic environment (amide pi-stacked,

pi-pi t stacked, pi-sigma, etc). It should be noted that binding site for protein is not similar for all synthesized molecules. All these data indicate that the core structure of our synthesized compounds is very cooperative with the protein.

## Conclusion

In conclusion, we developed a convenient method to synthesize 3-*m*-tolyl-5-arylidenthiazolidine- 2,4-dione derivatives by using morpholine as a catalyst. Molecular flexible docking studies have shown that our synthesized compounds are very active and some of them shown better binding affinity with the protein than the commercially available drugs, Epalrestat. These results inspire us to study the moiety even further and test these molecules for their biological activity. To find out more potent compound we plan to do pharmacokinetics study in near future.

## Supporting information

**S1 Fig. UV spectrum of 3-(*m*-tolyl) thiazolidine-2, 4- dione (4).**
(DOCX)

**S2 Fig. IR spectrum of 3-(*m*-tolyl) thiazolidine-2, 4- dione (4).**
(DOCX)

**S3 Fig. ^{1}H NMR spectrum of 3-(*m*-tolyl) thiazolidine-2, 4- dione (4).**
(DOCX)

**S4 Fig. ^{13}C NMR spectrum of 3-(*m*-tolyl) thiazolidine-2, 4- dione (4).**
(DOCX)

**S5 Fig. DEPT-135 spectrum of 3-(*m*-tolyl) thiazolidine-2, 4- dione (4).**
(DOCX)

**S6 Fig. UV of 5-(2-Methoxybenzylidene)-3-*m*-tolyl thiazolidine-2, 4- dione (7a).**
(DOCX)

**S7 Fig. IR spectrum of 5-(2-Methoxybenzylidene)-3-*m*-tolyl thiazolidine-2, 4- dione (7a).**
(DOCX)

**S8 Fig. ^{1}H NMR spectrum of 5-(2-Methoxybenzylidene)-3-*m*-tolyl thiazolidine-2, 4- dione (7a).**
(DOCX)

**S9 Fig. ^{13}C NMR spectrum of 5-(2-Methoxybenzylidene)-3-*m*-tolyl thiazolidine-2, 4- dione (7a).**
(DOCX)

**S10 Fig. DEPT-135 spectrum of 5-(2-Methoxybenzylidene)-3-*m*-tolyl thiazolidine-2, 4- dione (7a).**
(DOCX)

**S11 Fig. UV spectrum of 5-(2-Chlorobenzylidene)-3-*m*-tolyl thiazolidine-2, 4- dione (7b).**
(DOCX)

**S12 Fig. IR spectrum of 5-(2-Chlorobenzylidene)-3-*m*-tolyl thiazolidine-2, 4- dione (7b).**
(DOCX)

**S13 Fig. ^{1}H NMR spectrum of 5-(2-Chlorobenzylidene)-3-*m*-tolyl thiazolidine-2, 4- dione (7b).**
(DOCX)

**S14 Fig. <sup>13</sup>C NMR spectrum of 5-(2-Chlorobenzylidene)-3-*m*-tolyl thiazolidine-2, 4- dione (7b).**
(DOCX)

**S15 Fig. DEPT-135 spectrum of 5-(2-Chlorobenzylidene)-3-*m*-tolyl thiazolidine-2, 4- dione (7b).**
(DOCX)

**S16 Fig. UV spectrum of 5-(2-Nitrobenzylidene)-3-*m*-tolyl thiazolidine-2, 4- dione (7c).**
(DOCX)

**S17 Fig. IR spectrum of 5-(2-Nitrobenzylidene)-3-*m*-tolyl thiazolidine-2, 4- dione (7c).**
(DOCX)

**S18 Fig. <sup>1</sup>H NMR spectrum of 5-(2-Nitrobenzylidene)-3-*m*-tolyl thiazolidine-2, 4- dione (7c).**
(DOCX)

**S19 Fig. <sup>13</sup>C NMR spectrum of 5-(2-Nitrobenzylidene)-3-*m*-tolyl thiazolidine-2, 4- dione (7c).**
(DOCX)

**S20 Fig. DEPT-135 spectrum of 5-(2-Nitrobenzylidene)-3-*m*-tolyl thiazolidine-2, 4- dione (7c).**
(DOCX)

**S21 Fig. UV spectrum of 5-(3-Hydroxybenzylidene)-3-*m*-tolyl thiazolidine-2, 4- dione (7d).**
(DOCX)

**S22 Fig. <sup>1</sup>H NMR spectrum of 5-(3-Hydroxybenzylidene)-3-*m*-tolyl thiazolidine-2, 4- dione (7d).**
(DOCX)

**S23 Fig. DEPT-135 NMR spectrum of 5-(3-Hydroxybenzylidene)-3-*m*-tolyl thiazolidine-2, 4- dione (7d).**
(DOCX)

**S24 Fig. <sup>13</sup>C NMR spectrum of 5-(3-Hydroxybenzylidene)-3-*m*-tolyl thiazolidine-2, 4- dione (7d).**
(DOCX)

**S25 Fig. UV spectrum of 5-(4-Chlorobenzylidene)-3-*m*-tolyl thiazolidine-2, 4- dione (7e).**
(DOCX)

**S26 Fig. IR spectrum of 5-(4-Chlorobenzylidene)-3-*m*-tolyl thiazolidine-2, 4- dione (7e).**
(DOCX)

**S27 Fig. <sup>1</sup>H NMR spectrum of 5-(4-Chlorobenzylidene)-3-*m*-tolyl thiazolidine-2, 4- dione (7e).**
(DOCX)

**S28 Fig. <sup>13</sup>C NMR spectrum of 5-(4-Chlorobenzylidene)-3-*m*-tolyl thiazolidine-2, 4- dione (7e).**
(DOCX)

**S29 Fig. DEPT-135 spectrum of 5-(4-Chlorobenzylidene)-3-*m*-tolyl thiazolidine-2, 4-dione (7e).**
(DOCX)

**S30 Fig. Mechanism of the 3-aryl thiazolidine-2,4-dione synthesis (4).**
(DOCX)

**S31 Fig. Chemical structures of molecules optimized with DFT-B3LYP (6-31G, d) level of theory.**
(DOCX)

**S32 Fig. HOMO and LUMO structures of the optimized molecules.**
(DOCX)

**S33 Fig.**
(TIF)

## Acknowledgments

## Author Contributions

**Conceptualization:** Khorshada Jahan, Kaif Rashid Khan, Kawsari Akhter, Umme Kulsum Rowzatur Romman, Ershad Halim.

**Data curation:** Khorshada Jahan, Kaif Rashid Khan.

**Formal analysis:** Kaif Rashid Khan, Kawsari Akhter.

**Investigation:** Kaif Rashid Khan.

**Methodology:** Khorshada Jahan, Kaif Rashid Khan, Kawsari Akhter.

**Project administration:** Khorshada Jahan.

**Resources:** Khorshada Jahan.

**Software:** Kaif Rashid Khan.

**Supervision:** Khorshada Jahan, Kawsari Akhter, Umme Kulsum Rowzatur Romman.

**Validation:** Khorshada Jahan, Kawsari Akhter, Umme Kulsum Rowzatur Romman.

**Visualization:** Khorshada Jahan, Kawsari Akhter.

**Writing – original draft:** Khorshada Jahan, Kaif Rashid Khan.

**Writing – review & editing:** Khorshada Jahan, Kaif Rashid Khan, Kawsari Akhter, Umme Kulsum Rowzatur Romman, Ershad Halim.

## References

1. Abhishek KJ, Ankur V, Veerasamy R, Sushil KK, Ram KA. Recent developments and biological activities of thiazolidinone derivatives: a review. Bioorg Med Chem. 2012; 20(11): 3378–3395. https://doi.org/10.1016/j.bmc.2012.03.069 PMID: 22546204

2. Tihomir T, Lucija PM. Rhodanine as a scaffold in drug discovery: a critical review of its biological activities and mechanisms of target modulation. Expert Opin Drug Discov. 2012; 7(7): 549–560. https://doi.org/10.1517/17460441.2012.688743 PMID: 22607309

3.  Navriti C, Malkeet SB, Maninder K, Om S. Thiazolidine-2,4-dione derivatives: programmed chemical weapons for key protein targets of various pathological conditions. Bioorg Med Chem. 2015; 23(13): 2953–74. https://doi.org/10.1016/j.bmc.2015.03.071 PMID: 25890697

4.  Viral SJ, Dhagash KV, Ramaa CS. Thiazolidine-2,4-diones: progress towards multifarious applications. Bioorg Med Chem. 2013; 21(7): 1599–620. https://doi.org/10.1016/j.bmc.2013.01.029 PMID: 23419324

5.  Jwane SK, Singh VK, Namdeo KP, Prajpapti SK. Synthesis of some novel 2,4-thiazolidinedione derivatives and their biological screening as antidiabetic agents, Asian J Chem. 2009; 21(7): 5068–5072.

6.  Dietmar R, Rosanna M, Rosaria O, Maria GV. In vitro aldose reductase inhibitory activity of 5-benzyl-2,4-thiazolidinediones. Bioorg Med Chem 2006; 14(2): 567–74. https://doi.org/10.1016/j.bmc.2005.08.056 PMID: 16202614

7.  Havrylyuka D, Zimenkovskya B, Lesyla R. Synthesis and anticancer activity of novel nonfused bicyclic thiazolidinone derivatives. Phosphorus, sulfur, and silicon and the related elements, 2009; 184(3): 638–650. https://doi.org/10.1080/10426500802247563.

8.  Ceriello A. Thiazolidinediones as anti-inflammatory and antiatherogenic agents. Diabetes Metab Res Rev. 2008; 24(1): 14–26. https://doi.org/10.1002/dmrr.790 PMID: 17990280

9.  Deepak KA, Poonam L, Sanjiv A, Chetan S, Kamal RA, Om P. Synthesis of new pyrazolyl-2, 4-thiazolidinediones as antibacterial and antifungal agents. Org Med Chem Lett. 2011; 1: 1–15. https://doi.org/10.1186/2191-2858-1-1 PMID: 22373059

10.  Oya BD, Özen Ö, Arzu M, Nurten A, Onur A, Engin K, et al. Synthesis and antimicrobial activity of some new thiazolyl thiazolidine-2,4-dione derivatives. Bioorg Med Chem. 2007; 15(18): 6012–6017. https://doi.org/10.1016/j.bmc.2007.06.049 PMID: 17618124

11.  Dirk AH, Lisa TC, Tammy JC, David JH, Stephen FR, Dennis TT, et al. New benzylidenethiazolidine-diones as antibacterial agents. Bioorg Med Chem Lett. 2003; 13(21): 3771–3773. https://doi.org/10.1016/j.bmcl.2003.07.010 PMID: 14552776

12.  Zimenkovskii BS, Kutsyk RV, Lesyk RB, et al. Synthesis and antimicrobial activity of 2,4-dioxothiazolidine-5-acetic acid amides. Pharm Chem J. 2006; 40(6): 303–306.

13.  Pattan S, Kedar M, Pattan J, et al. Synthesis and evaluation of some novel 2,4-thiazolidinedione derivatives for antibacterial, antitubercular and antidiabetic activities. Indian J Chem. 2012; 51B: 1421–1425.

14.  Robin EB. Thiazolidinediones: Pleiotropic drugs with potent anti-inflammatory properties for tissue protection. Hepatol. Res. 2005; 33(2): 167–170. https://doi.org/10.1016/j.hepres.2005.09.027 PMID: 16198619

15.  Raymond AD, Dallas CJ. Emerging roles of PPARS in inflammation and immunity. Nat. Rev. Immunol. 2002; 2: 748–759. https://doi.org/10.1038/nri912 PMID: 12360213

16.  Mercedes R, Andrew CL, Timothy MW, Carolyn JK, Christopher KG. The peroxisome proliferator-activated receptor-γ is a negative regulator of macrophage activation. Nature. 1998; 391: 79–82. https://doi.org/10.1038/34178 PMID: 9422508

17.  Chengyu J, Adrian TT, Brian SC, PPAR-γ agonists inhibit production of monocyte inflammatory cytokines. Nature. 1998; 391: 82–86. https://doi.org/10.1038/34184 PMID: 9422509

18.  Anna G. Effect of the new thiazolidinedione-pioglitazone on the development of oxidative stress in liver and kidney of diabetic rabbits Life Sciences. 2003; 74(5): 553–562. https://doi.org/10.1016/j.lfs.2003.03.004 PMID: 14623026

19.  Devinyak O, Zimenkovsky B, Lesyk R. Biologically Active 4-Thiazolidinones: A Review of QSAR Studies and QSAR Modeling of Antitumor Activity. Curr Top Med Chem. 2012; 12(24): 2763–2784. https://doi.org/10.2174/1568026611212240006 PMID: 23368102

20.  Tomasic T, Masic LP, Rhodanine as a Privileged Scaffold in Drug Discovery. Curr Med Chem. 2009; 16(13): 1596–1629. https://doi.org/10.2174/092986709788186200 PMID: 19442136

21.  Sherida LJ, Li-Hsing C, Rebecca H, Mojgan S, Alexei S, Naomi JHC, et al. Rhodanine Derivatives as Selective Protease Inhibitors Against Bacterial Toxins. Chem Biol Drug Des. 2008; 71(2): 131–139. https://doi.org/10.1111/j.1747-0285.2007.00617.x PMID: 18221310

22.  Kiran FS, Suryakant BS, Gopal KK, et al. Alum catalyzed simple and efficient synthesis of 5-arylidene-2,4-thiazolidinedione in aqueous media. Chem Lett Rev. 2010; 3: 17–21. https://doi.org/10.1080/17518250903478345.

23.  Mahalle S, Ligampalle D, Mane R. Microwave-Assisted Synthesis of Some 2,4-Thiazolidinedione Derivatives. Heteroatom Chem. 2009; 20(3): 151–156. https://doi.org/10.1002/hc.

24.  Bruno G, Costantino L, Curinga C, Maccari R, Monforte F, Nicolo F, et al. Synthesis and aldose reductase inhibitory activity of 5-arylidene-2,4-thiazolidinedione. Bioorg Med Chem. 2002; 10(4): 1077–1084. https://doi.org/10.1016/s0968-0896(01)00366-2 PMID: 11836118

25. Jian-Feng Z, Feng-Xia Z, Yuan-Zhi S, Yu-Lan Z. Synthesis of 5-arylalkylidenerhodanines catalyzed by tetrabutylammonium bromine in water under microwave irradiation. Arkivoc. 2006; 14: 175–180.

26. Umesh RP, Dhanaji VJ, Rahul AW, Dinesh LL. Ramrao AM. Synthesis of 5-arylidene-2,4-thiazolidine-diones by Knoevenagel condensation catalyzed by baker's yeast. New J Chem. 2011; 35: 49–51. https://doi.org/10.1039/C0NJ00691B.

27. Abdolhamid A, Mohammad MK, Ali E. A solvent-free protocol for the green synthesis of arylalkylidene rhodanines in a task-specific ionic liquid. Can J Chem. 2010; 88(6): 514–518. https://doi.org/10.1139/V10-011.

28. Jawale DV, Pratap UR, Lingampalle DL, Mane RA. Dicationic ionic liquid mediated synthesis of 5-arylidine-2,4-thiazolidinediones. Chin J Chem. 2011; 29: 942–946. https://doi.org/10.1002/cjoc.201190192.

29. Gong K, He ZW, Xu Y, Fang D, Liu ZL. Synthesis of 5-benzylidene rhodanine derivatives catalyzed by 1-butyl-3-methyl imidazolium hydroxide in water. Monatsh Chem. 2008; 139: 913–915. https://doi.org/10.1007/s00706-008-0871-y.

30. Shelke KF, Sapkal SB, Madje BR, Shingate BB, Shingare MS. Ionic liquid promoted an efficient synthesis of 5-arylidene-2,4-thiazolidinedione. Bull Catal Soc India. 2009; 8: 30–34.

31. Yang DH, Chen ZC, Chen SY, Zheng QG. Organic reactions in ionic liquids; ionic liquid-accelerated three-component reaction: a rapid one-pot synthesis of 3-alkyl-5-(Z)-arylmethylidene-1,3-thiazolidine-2,4-diones. Synthesis. 2003; 1891–1894. https://doi.org/10.1055/s-2003-40980.

32. Malihe A, Naser F, Hoda P, Alireza KA, Ahmadreza B. Copper (II)-complex functionalized magnetite nanoparticles: a highly efficient heterogeneous nanocatalyst for the synthesis of 5-arylidenthiazolidine-2,4-diones and 5-arylidene-2-thioxothiazolidin-4-one. Transit Met Chem, 2017, 42: 543–552. https://doi.org/10.1007/s11243-017-0159-3.

33. Ahmed MG, Romman UKR, Akhter K, Jahan K, Bhuiyan MNH, Halim ME. Synthesis of substituted tetrahydrochromenes by the reactions of α, β-unsaturated cyanoesters with dimedone/1,3-cyclohexane-dione. Syn Commun. 2011; 41: 2822–2827. https://doi.org/10.1080/00397911.2010.515346.

34. Akhter K, Jahan K, Romman UKR, Ahmed MG, Rahman MS, Al-Amin M. A Green Approach to Synthesize Dihydropyrimidinone Derivatives by Using Anhydrous $ZnCl_2$ Catalyst Under Refluxing Condition in Heptane-Toluene Medium via Biginelli Reaction. Asian J Chem. 2015; 27(7), 2624–2626. https://doi.org/10.14233/ajchem.2015.18615.

35. Rifat S, Jahan K, Romman UKR, Akhter K, Halim ME. A Green Approach to Synthesize and in vitro Antimicrobial Activity of Indeno-Imidazole Derivatives and Ninhydrin-Nucleophile Adducts. Asian J Chem. 2016; 28(7),1611–1616. https://doi.org/10.14233/ajchem.2016.19775.

36. Akhter K, Jahan K, Halim ME, Shefa S, Rifat S, Khan KR, Ahmed SM, Romman UKR. Synthesis of 1-phenyl-3,4-dihydropyrimidine-2(1H)-ones derivatives under solvent free condition and study of their antimicrobial activity. Bangladesh J. Sci. Ind. Res. 2019; 54(1), 47–54. https://doi.org/10.3329/bjsir.v54i1.40730.

37. Peng Y-H, Lin C-H, Hsieh H-P, Wu S-Y, Crystal structure of Human PPAR-gamma ligand domain complexed with a potent and selective agonist. Protein Data Bank. 2011. https://doi.org/10.2210/pdb3gbk/pdb